# Specific Inhibition of Histone Deacetylase 8 Reduces Gene Expression and Production of Proinflammatory Cytokines *in Vitro* and *in Vivo**

Suzhao Li[‡], Gianluca Fossati[§], Carlo Marchetti[¶], Daniela Modena[§], Pietro Pozzi[§], Leonid L. Reznikov[‡], Maria Luisa Moras[§], Tania Azam[‡], Antonio Abbate[¶], Paolo Mascagni[§], and Charles A. Dinarello[‡‖1]

From the [‡]Department of Medicine, University of Colorado Denver, Aurora, Colorado 80045, [§]Italfarmaco, S.p.A., Cinisello Balsamo 20092, Italy, the [¶]Department of Medicine, Virginia Commonwealth University, Richmond, Virginia 23298, and the [‖]Department of Medicine, Radboud University Medical Centre, 6525 HP Nijmegen, The Netherlands

**Background:** Low concentrations of HDAC inhibitors suppress inflammation, but HDAC inhibitors are toxic at higher concentrations.
**Results:** ITF3056 specifically inhibits HDAC8 activity and reduces proinflammatory cytokine production from human blood monocytes and *in vivo* but lacks cell toxicity.
**Conclusion:** Specific inhibition of HDAC8 reduces inflammation with low cell toxicity.
**Significance:** Inhibition of specific HDACs is preferred for treating inflammatory diseases, with fewer side effects.

ITF2357 (generic givinostat) is an orally active, hydroxamic-containing histone deacetylase (HDAC) inhibitor with broad anti-inflammatory properties, which has been used to treat children with systemic juvenile idiopathic arthritis. ITF2357 inhibits both Class I and II HDACs and reduces caspase-1 activity in human peripheral blood mononuclear cells and the secretion of IL-1$\beta$ and other cytokines at 25–100 nM; at concentrations >200 nM, ITF2357 is toxic *in vitro*. ITF3056, an analog of ITF2357, inhibits only HDAC8 (IC$_{50}$ of 285 nM). Here we compared the production of IL-1$\beta$, IL-1$\alpha$, TNF$\alpha$, and IL-6 by ITF2357 with that of ITF3056 in peripheral blood mononuclear cells stimulated with lipopolysaccharide (LPS), heat-killed *Candida albicans*, or anti-CD3/anti-CD28 antibodies. ITF3056 reduced LPS-induced cytokines from 100 to 1000 nM; at 1000 nM, the secretion of IL-1$\beta$ was reduced by 76%, secretion of TNF$\alpha$ was reduced by 88%, and secretion of IL-6 was reduced by 61%. The intracellular levels of IL-1$\alpha$ were 30% lower. There was no evidence of cell toxicity at ITF3056 concentrations of 100–1000 nM. Gene expression of TNF$\alpha$ was markedly reduced (80%), whereas IL-6 gene expression was 40% lower. Although anti-CD3/28 and *Candida* stimulation of IL-1$\beta$ and TNF$\alpha$ was modestly reduced, IFN$\gamma$ production was 75% lower. Mechanistically, ITF3056 reduced the secretion of processed IL-1$\beta$ independent of inhibition of caspase-1 activity; however, synthesis of the IL-1$\beta$ precursor was reduced by 40% without significant decrease in IL-1$\beta$ mRNA levels. In mice, ITF3056 reduced LPS-induced serum TNF$\alpha$ by 85% and reduced IL-1$\beta$ by 88%. These data suggest that specific inhibition of HDAC8 results in reduced inflammation without cell toxicity.

DNA is tightly wrapped around nuclear histones and maintained in a state of deacetylation by histone deacetylases (HDACs),[2] silencing gene expression. In humans, there are 18 HDACs divided into classes based on their dependence on zinc for enzyme activity (1). Class I (HDAC1, -2, -3, and -8) and Class II (HDAC4, -5, -6, -7, -9, -10, and -11) are zinc-dependent enzymes, whereas class III (sirtuins 1–7) are NAD$^+$-dependent (2, 3). Although HDACs deacetylate the highly conserved N-terminal lysines on nuclear histones, HDACs also target cytosolic proteins, such as transcription factors and proteins, that regulate cell proliferation, migration, and death (4). HDAC inhibitors hyperacetylate signal transducers and activators of transcription (STAT) (5) and NF$\kappa$B, both of which are associated with decreased inflammation (6).

Synthetic inhibitors of HDACs are orally active and well tolerated and have been used widely in medicine (reviewed in Ref. 7). Although synthetic HDAC inhibitors were developed to increase pro-apoptotic genes in cancer (8), we have studied HDAC inhibitors as anti-inflammatory agents using concentrations significantly lower than those used for anti-tumor effects. In both *in vitro* cellular assays as well as in animal models of inflammatory and autoimmune diseases, low concentrations of HDAC inhibitors reduce cytokine production and severity of disease. ITF2357 (generic givinostat) is a hydroxamic acid-containing, orally active inhibitor that is anti-inflammatory in the low nanomolar range, either *in vitro* or *in vivo* (9–16). For example, in mice with inducible (17) or spontaneous (6) diabetes, a low dose of oral ITF2357 of 1.5 mg/kg/day protected the insulin-producing islets as well as the incidence of clinical diabetes. In a Phase I trial in healthy males, oral givinostat reduced the production of proinflammatory cytokines from whole blood cultures (18). Children with systemic juvenile idiopathic arthritis have been successfully treated with givinostat (19, 20).

[2] The abbreviations used are: HDAC, histone deacetylase; PBMC, peripheral blood mononuclear cell; LDH, lactate dehydrogenase; PI, propidium iodide.

In addition, patients with hematopoietic bone marrow transplantation have been treated with a related HDAC inhibitor vorinostat, and a significant reduction in graft *versus* host disease was observed (21). Based on *in vitro* data (22), HDAC inhibitors are also being tested in HIV-1 infections to decrease the population of latently infected T-cells but also to reduce in indolent inflammation of the disease (23–26).

Givinostat and vorinostat are pan-HDAC inhibitors in that they inhibit Class I and Class II HDACs. In developing more specific HDAC inhibitors, analogues of givinostat (ITF2357) were generated. In the present study, we compared the effect on cytokine production by an HDAC8-specific inhibitor ITF3056 with that of the pan-HDAC inhibitor ITF2357. Freshly obtained human peripheral blood mononuclear cells (PBMCs) were stimulated with LPS (for TLR4 responses), heat-killed *Candida albicans* (for broad stimulation by TLRs and C-type lectin receptors as well as NOD-like receptors (27)) or anti-CD3 in combination with anti-CD28 antibodies (for T-cell responses); the effect of the two analogues on cytokine production was determined. In addition, circulating TNFα and IL-1β were measured in mice treated with ITF2357 or ITF3056 prior to LPS.

## EXPERIMENTAL PROCEDURES

*Reagents*—ITF2357 and ITF3056 were synthesized at Italfarmaco (Cinisello Balsamo, Italy), and purity was confirmed by high performance liquid chromatography. ITF2357 was dissolved in water and kept at room temperature (11). ITF3056 was dissolved in DMSO to a concentration of 20 mM, divided into aliquots, and stored at −80 °C. Frozen aliquots of ITF3056 (20 mM in 100% DMSO) were freshly thawed and further diluted in warm RPMI to different concentrations for experiments. The concentrations used in these studies were 1000, 500, 200, 100, 50, and 25 nM. For 1000 nM ITF3056, the final concentration of DMSO in cell culture is 0.005%. In parallel, 0.005% DMSO alone in RPMI was used as vehicle control, and no effect was observed compared with RPMI alone. Lipopolysaccharide (LPS) *Escherichia coli* (055:B5) was purchased from Sigma. Lactate dehydrogenase (LDH) cytotoxicity assay kit was purchased from Biovision (Mountain View, CA). All related antibodies for electrochemiluminescence (ECL) or ELISA were from R&D Systems (Minneapolis, MN). Heat-killed *C. albicans* UC820 was kindly provided by Professor Mihai Netea (Radboud University Medical Centre, Nijmegen, The Netherlands). Anti-human CD3 and anti-human CD28 antibodies were purchased from eBioscience (San Diego, CA).

*PBMC Cultures*—The study was approved by the Colorado Medical Institutional Review Board. Venous blood from healthy consenting donors was drawn into lithium heparin-containing tubes, and PBMCs were isolated using centrifugation over Ficoll-Hypaque cushions as described previously (11). Cells were washed three times with 0.9% saline and resuspended in RPMI at $5 \times 10^6$/ml. For LPS stimulation, $0.5 \times 10^6$ cells were seeded per well in 96-flat bottom well plates and cultured in a total of 200 µl of RPMI for 24 h, with or without 10 ng/ml LPS or increasing concentrations of the analogues. For cultures with *Candida* or anti-CD3/CD28, $0.5 \times 10^6$ cells were seeded per well in 96-round bottom well plates and cultured in

a total of 200 µl of RPMI with 10% pooled human serum for 5 days, with or without *Candida* ($10^6$ colonies/ml) or 5 µg/ml anti-CD3 plus 1 µg/ml anti-CD28 as stimuli (28, 29), in the presence of increasing concentrations of the analogues. The HDAC inhibitors were added 30 min before the stimuli. After incubation times were completed, supernatants were collected by centrifugation at 1000 rpm for 5 min and stored at −80 °C. Cells remaining in the wells were lysed in 100 µl of 0.5% Triton X-100 in water and stored at −80 °C for later analysis.

*Cytokine Measurement*—Supernatant human mature IL-1β, TNFα, IL-6, IFNγ, and intracellular IL-1α were measured with ECL assays (Bioveris, Gaithersburg, MD) as described previously (11, 30, 31). Supernatant and intracellular human IL-1β precursor and mouse serum TNFα were measured by specific ELISAs (R&D Systems). Total IL-1β was calculated by adding extracellular and intracellular compartments of supernatant and lysates for mature as well as precursor IL-1β. The percentage of each compartment for either mature or precursor IL-1β was then determined for each concentration of HDAC inhibitor.

*Enzymatic Assay for HDAC Activity*—Recombinant human HDAC enzymes (HDAC1–10) were purchased from BPS (San Diego, CA). HDAC11 was purchased from Enzo Life Sciences (Farmingdale, NY). Activity of HDAC1, -2, -3, -6, -10, and -11 was assayed using the Fluor de Lys deacetylase substrate (Enzo Life Sciences). HDAC8 activity was assayed using Fluor de Lys Green deacetylase substrate (Enzo Life Science). $N^{\epsilon}$-Trifluoro-acetyl-L-lysine was used to assay activity of HDAC 4, 5, 7, and 9. Recombinant enzymes were preincubated with ITF2357 or ITF3056 at 30 °C in a volume of 25 µl in wells of a microtiter plate. After a brief incubation, 25 µl of substrate was added, and the fluorescent signal was generated by the addition of 50 µl of developer (Fluor de Lys Developer (Enzo Life Science) containing 2 µM Trichostatin A (Sigma-Aldrich). For each assay, the amount of enzyme, incubation times, assay buffer, and concentration of the substrates were optimized. Positive control for enzyme activity consisted of enzyme plus substrate without ITF2357 or ITF3056. The fluorescence signal was detected using a Victor multilabel plate reader (PerkinElmer Life Sciences).

*Caspase-1 Activity Assay*—Human PBMCs from four donors were stimulated with LPS (10 ng/ml) for 4 and 24 h. Based on the reduction by ITF2357 and ITF3056 of LPS-induced IL-1β production and secretion, 25 nM ITF2357 and 1000 nM ITF3056 were selected as the optimal concentrations to assess effects on caspase-1 activity. ITF2357 (25 nM) or ITF3056 (1000 nM) were added 30 min prior to LPS. After the supernatant was removed, the cells were lysed using radioimmune precipitation assay buffer (Sigma-Aldrich) containing a mixture of protease inhibitors and centrifuged at 12,000 rpm for 20 min at 4 °C. The supernatants were assayed for protein content using the Bio-Rad method. Protein was processed for caspase-1 activity using the fluorogenic substrate A2452 (Sigma-Aldrich). The fluorescence was reported as arbitrary fluorescence units generated by 1 µg of sample/min (fluorescence/µg/min). The data were expressed as the percentage change in caspase-1 activity present in the lysates of LPS-stimulated PBMCs incubated with analogues, with the lysates from LPS only set as 100%.

*Assays for Cytotoxicity*—Three assays were used to compare the cytotoxic effects of ITF2357 with those of ITF3056. LDH release was measured in supernatants from freshly obtained PBMCs cultured in 96-flat bottom well plates for 24 h in the presence of LPS (10 ng/ml) without fetal calf serum as described previously using the LDH cytotoxicity assay kit from Biovision (Mountain View, CA) (22). The percentage of LDH release was calculated according to the manufacturer's instructions. In addition, cell viability was assessed in PBMCs cultured in RPMI supplemented with 1% FCS in the presence of LPS (10 ng/ml) at 400,000 cells/ml in a 96-flat bottom well plate for 24 h. At the end of incubation, cell viability was determined by the CellTiter 96® Aqueous One solution cell proliferation assay (Promega, Madison, WI) according to the manufacturer's instructions. We also assessed cell viability in PBMC isolated from buffy coat cells of human citrated blood. PBMCs isolated from buffy coats were seeded at 500,000 cells/well (96-flat bottom well plate) in RPMI with 10% FCS and incubated for 72 h in the presence of increasing concentrations of ITF2357 or ITF3056 using the CellTiter assay as described above.

*Annexin V Staining for Monocyte Apoptosis*—Monocytes were isolated from fresh PBMCs by magnetic separation (Monocyte Isolation Kit II, Miltenyi Biotec, Germany) and resuspended in RPMI containing 10% FCS. Purified monocytes were seeded at 250,000 cells/well and incubated in the presence of increasing concentrations of ITF2357 or ITF3056 with LPS (10 ng/ml). After 24 h, the cells were labeled with annexin V-FLUOS (Roche Applied Science) and propidium iodide (PI) following the manufacturer's instructions. The percentages of annexin V-positive and annexin V/PI-double-positive cells were determined by flow cytometric analysis.

*Caspase-3/7 Determinations for Monocyte Apoptosis*—Monocytes, isolated as described above, were incubated at 50,000 cells/well in 96-flat bottom well plates in the presence of increasing concentrations of ITF2357 or ITF3056 with LPS (10 ng/ml) for 24 h of incubation. The activity of caspase-3/7 was then determined by the Apo-ONE homogeneous caspase-3/7 assay (Promega), and the amount of fluorescence was detected by a fluorimetric plate reader (Victor-2, PerkinElmer Life Sciences).

*Steady State mRNA Levels and Real-time PCR*—To obtain sufficient RNA for analysis of steady state mRNA levels of different cytokines, $3 \times 10^6$ cells were seeded per well in 24-well plates and cultured in a total of 1200 μl of RPMI for 20 h, with or without 10 ng/ml LPS and increasing concentrations of the analogues. The HDAC inhibitors were added 30 min before the addition of LPS. After 20 h of incubation at 37 °C, the supernatants were collected, and cytokine levels were measured. The cells were washed with PBS and lysed in RLT Plus lysis buffer. Total RNA was collected with the RNeasy mini plus kit from Qiagen (Hilden, Germany). Approximately 300–500 ng of total RNA was reverse-transcribed using the Superscript first-strand synthesis system to obtain the cDNA (Invitrogen). Real-time PCR was then performed on a 7300 Real-time PCR system with a cycle of 40 using Power SYBR Green PCR Master Mix (Applied Biosystems). PCR using GAPDH-specific primers as an internal control was performed for each RNA sample. The forward primer for IL-1β real-time PCR was GCA CGA TGC ACC TGT ACG AT, and the reverse primer was AGA CAT

CAC CAA GCT TTT TTG CT. The forward primer used for TNFα real-time PCR was CCC AGG CAG TCA GAT CAT CTT C, and the reverse primer was AGC TGC CCC TCA GCT TGA. The forward primer for IL-6 was GGT ACA TCC TCG ACG GCA TCT, and the reverse primer was GTG CCT CTT TGC TGC TTT CAC. For GAPDH, the forward primer was TGC ACC ACC AAC TGC TTA GC, and the reverse primer was GGC ATG GAC TGT GGT CAT GAG.

The relative ratio of the mRNA from each cytokine gene to internal control (GAPDH) was calculated as: $1/2^{\Delta Ct}$ (cytokine gene minus the internal control gene). The -fold change of mRNA from treated cells over the negative control (untreated cells) was further calculated based on the relative ratio. Levels of LPS-induced mRNA were set at 100%, and the percentage change for each concentration of ITF2357 or ITF3056 was calculated. The data are depicted as the mean percentage change compared with LPS alone.

*Animal Studies*—Animal protocols were approved by the University of Colorado Health Sciences Center Animal Care and Use Committee. C57BL/6 mice were purchased from Charles River (Reading, MA) and housed in the animal facility for at least 5 days before use. For the comparison study, ITF2357 at 10 mg/kg was administered orally as reported previously (11), and ITF3056 was injected intraperitoneally. One hour after administration of the compounds, the animals were treated intraperitoneally with LPS from *Salmonella typhimurium* (Sigma-Aldrich) at a dose of 2.5 mg/kg. 90 min after the LPS treatment, mice were sacrificed, and sera were collected and stored at −80 °C until further analysis of cytokine productions. A dose-response study of ITF3056 at 4, 8, and 16 mg/kg was performed in mice injected intraperitoneally with LPS from *E. coli* (055:B5) (Sigma-Aldrich) at 10 mg/kg. After 4 h, the serum was collected for cytokine levels. Another dose study of ITF3056 at 1 and 5 mg/kg used a lower dose of LPS (2.5 mg/kg) given intraperitoneally after ITF3056 injection. 4 h later, the mice were sacrificed, and blood was collected. Blood was collected in EDTA, separated into plasma for cytokine levels, or diluted in RPMI for whole blood culture as described previously (33).

*Statistical Analysis*—Results are expressed as mean ± S.E. (*n* is noted in the figure legends). Statistical significance was evaluated with Student's two-tailed *t* test.

## RESULTS

*A Comparison of the Effect of ITF2357 with That of Its Analog ITF3056 on LPS-induced IL-1β Production and Secretion*—To find more selective HDAC inhibitors, analogues of ITF2357 were generated and assessed for inhibition of enzymatic activity (34). Analog ITF3056 was highly specific for inhibition of HDAC8, with IC$_{50}$ at 285 nM with no significant inhibition of other HDACs (Table 1). By comparison, ITF2357 primarily inhibits Class I and II HDACs, and, as shown, ITF2357 inhibits HDAC1 and -3, with an IC$_{50}$ of 198 and 157 nM, respectively.

Fig. 1*A* illustrates the different compartments of mature and precursor IL-1β produced in LPS-stimulated PBMC. We used specific, non-cross-reacting ELISAs to measure the mature and precursor forms of IL-1β and calculated the percentage in each compartment of the total. As shown in Fig. 1*B*, ITF2357 suppressed total LPS-induced IL-1β production robustly com-

**TABLE 1**

Inhibition ($IC_{50}$) of HDACs by ITF2357 or the analogue ITF3056

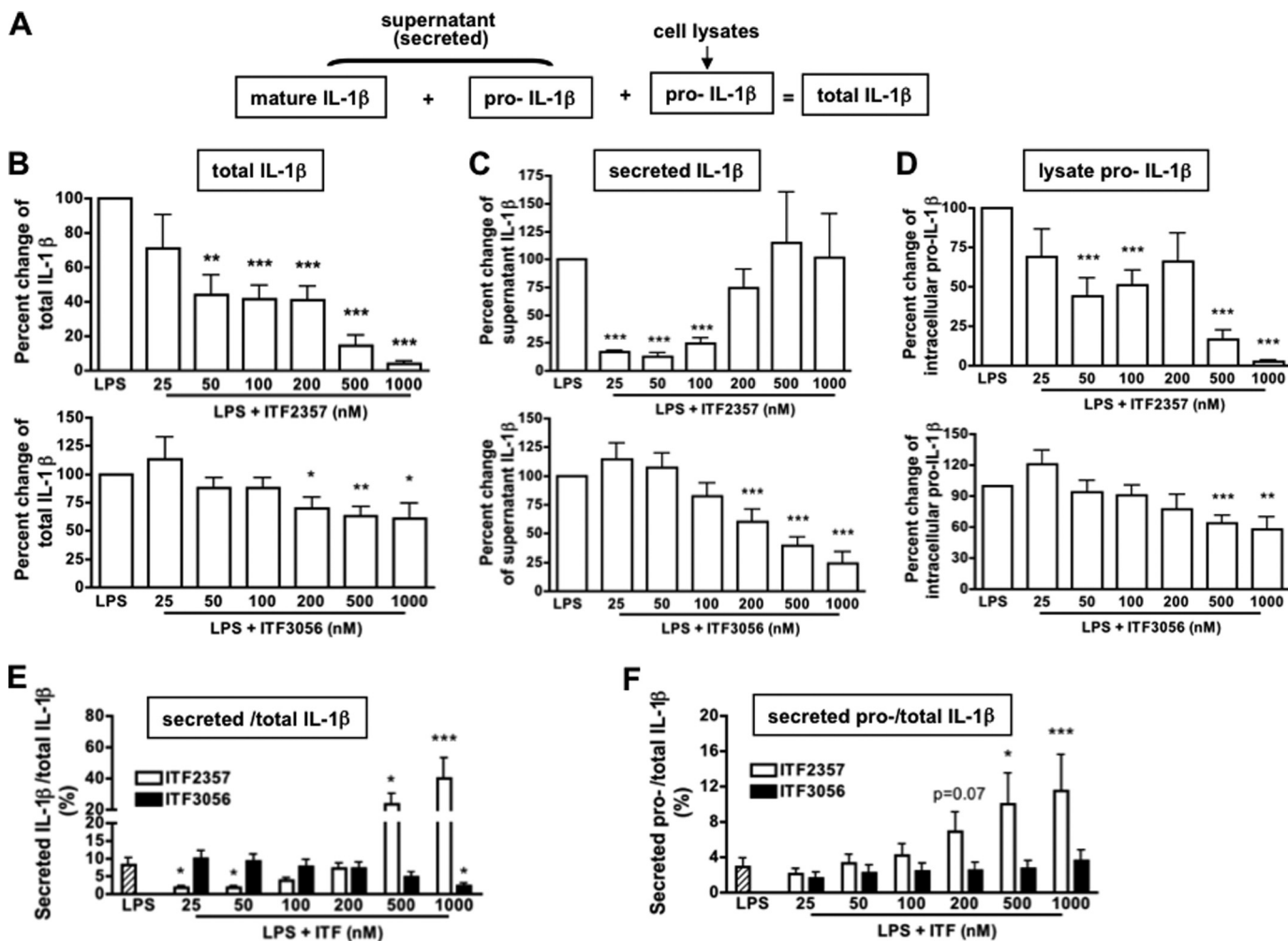| ITF | hHDAC1 | hHDAC2 | hHDAC3 | hHDAC8 | hHDAC4 | hHDAC5 | hHDAC7 | hHDAC9 | hHDAC6 | hHDAC10 | hHDAC11 |
|------|--------|--------|--------|--------|--------|--------|--------|--------|--------|---------|---------|
| 2357 | 198 | 325 | 157 | 854 | 1059 | 532 | 524 | 541 | 315 | 340 | 292 |
| 3056 | 2033 | >3000 | >3000 | 285 | >10000 | >10000 | >10000 | >10000 | >3000 | >3000 | >3000 |



FIGURE 1. **Comparison of the effect of ITF2357 with that of the analog ITF3056 on LPS-induced IL-1β production in PBMC cultures.** *A*, diagram depicts LPS (10 ng/ml) stimulation of PBMC cultures from nine healthy subjects. Shown is IL-1β as measured in the different compartments using specific assays for mature IL-1β and the IL-1β precursor. *B*, mean ± S.E. dose-response of total IL-1β as a percentage change of ITF2357 (*top*) or ITF3056 (*bottom*). *C*, mean ± S.E. percentage change of secreted mature IL-1β as measured in the supernatants. Data are derived from cultures shown in *B*. *D*, mean ± S.E. percentage change of lysate containing the intracellular IL-1β precursor in cultures shown in *B*. *E*, mean ± S.E. of the percentage of the secreted mature IL-1β specific over the total IL-1β of data derived from *B–D*. *F*, mean ± S.E. of the percentage of the IL-1β precursor as measured in the supernatants over total IL-1β. ***, $p < 0.001$; **, $p < 0.01$; *, $p < 0.05$, compared with LPS alone.

pared with the reduction by ITF3056. At 25, 50, and 100 nM, ITF2357 reduced IL-1β secretion more than 70% (Fig. 1*C*), consistent with previous studies (11). However, at concentrations of 200, 500, or 1000 nM, we observed greater variability in donor responses (Fig. 1*C*, *top*). In contrast, ITF3056 exhibited a linear reduction in IL-1β secretion from 200 to 1000 nM (Fig. 1*C*, *bottom*).

We next compared the effect of ITF2357 and 3056 on the level of the intracellular IL-1β precursor. From previous studies (35, 36), in freshly obtained human PBMCs, ~10–15% of the total intracellular content of the IL-1β precursor is processed by caspase-1 and secreted during a 24-h culture of monocytes, whereas most of the precursor remains unprocessed in the

cells. This was also observed in the present study. Although at 50 and 100 nM, ITF2357 reduced the level of the IL-1β precursor by 50% (Fig. 1*D*, *top*), at 500 and 1000 nM, the reduction is probably due to cell death (11). In contrast, there was a linear reduction of the precursor by the analog ITF3056, which reached statistical significance at 500 and 1000 nM (Fig. 1*D*, *bottom*). These data indicate that ITF3056 at 500–1000 nM concentrations reduces the synthesis of IL-1β and are consistent with the reduction in LPS-induced mRNA (see Fig. 4*B*).

We further compared the effects of ITF2357 and ITF3056 on the efficiency of IL-1β secretion by calculating the percentage of secreted IL-1β over total IL-1β production (Fig. 1*E*). Although ITF2357 inhibited the percentage of secreted IL-1β at
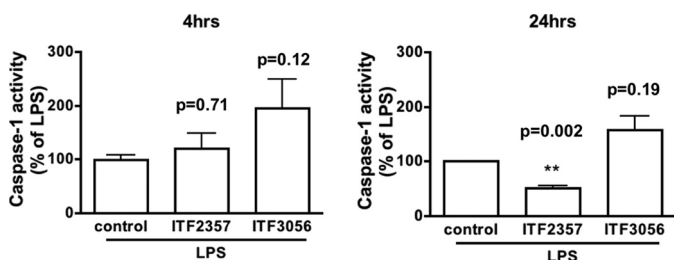
FIGURE 2. **Differential effects of ITF2357 and ITF3056 on caspase-1 activity.** Mean ± S.E. of caspase-1 activity in PBMC lysates 4 h (*left*) and 24 h (*right*) after LPS (10 ng/ml). Caspase-1 activity is expressed as the percentage change of the mean value of each assay with LPS set at 100% (see "Experimental Procedures" for details). ITF2357 (25 nM) and ITF3056 (1000 nM) were added 30 min before LPS; the concentrations were based on the data shown in Fig. 1. $n = 4$ donors; significant ($p < 0.05$) or non-significant ($p > 0.05$) $p$ values compared with control condition are provided *above* the corresponding graph bars. ***, $p < 0.001$; **, $p < 0.01$; *, $p < 0.05$, compared with control.

25 and 50 nM, with increasing concentrations, there was more IL-1$\beta$ compared with LPS without ITF2357. In contrast, ITF3056 reduced the percentage of secreted IL-1$\beta$ in a linear fashion, which reached significance at 1000 nM ($p < 0.05$).

We next measured the level of caspase-1 activity in the lysates of PBMC after LPS stimulation in the presence of ITF2357 compared with ITF3056. As shown in Fig. 2, ITF2357 reduced caspase-1 activity by ~50% 24 h after LPS ($p = 0.002$), whereas ITF3056 showed no inhibition of caspase-1 activity ($p = 0.19$). At 4 h following LPS, both ITF2357 and ITF3056 showed no significant effect on caspase-1 activity when compared with LPS alone.

From our previous study, ITF2357 at concentrations of 250 nM or higher can be injurious to PBMCs (11); thus, the percentage of secreted IL-1$\beta$ over total IL-1$\beta$ production at 500 and 1000 nM could be related to increased release of the IL-1$\beta$ precursor from the disrupted cell membrane and cell death. The amount of secreted precursor IL-1$\beta$ was calculated as the percentage of total IL-1$\beta$ production (Fig. 1*F*). ITF2357 at 500 and 1000 nM specifically enhanced precursor IL-1$\beta$ release from the cell but not at lower concentrations (<200 nM).

We also examined the levels of intracellular IL-1$\alpha$ in cell lysates. Immunoassays for IL-1$\alpha$ detect both the precursor and processed forms of the cytokine. ITF2357 reduced IL-1$\alpha$ levels significantly from 25 nM (35% reduction) to 200 nM (31% reduction). However, the reductions of 80 and 90% at 500 and 1000 nM are probably due to cell death. The analog ITF3056 exhibited a linear reduction, reaching statistical significance at 500 nM (24% reduction) and 1000 nM (32% reduction).

*Lack of Cytotoxicity by HDAC-8 Inhibition*—We used the release of LDH to first assess the cytotoxic effects of these analogues. As shown in Fig. 3*A*, ITF2357 resulted in the release of LDH at 200, 500, and 1000 nM, whereas ITF3056 at these same concentrations had no effect on LDH release. Similar findings were observed in PBMCs isolated from either fresh blood or buffy coat cells using a cell proliferation assay. For LPS-stimulated PBMC obtained from fresh blood, 87% of cells were viable with 123 nM ITF2357 but only 63% viable at 370 nM and only 52.5% viable at 1000 nM. In contrast, more than 93% cells were viable even at 1000 nM ITF3056. For PBMC obtained from buffy coats, at 123, 370, and 1111 nM ITF2357, there were correspondingly 63, 40, and 32% viable cells, whereas 87% of cells

remained viable at 1111 nM ITF3056. Because monocytes are the major producers of the cytokines induced by LPS, we determined annexin V staining in isolated monocytes (Fig. 3*B*) as well as activation of caspase-3/7 (Fig. 3*C*). Consistently, ITF3056 lacked cell toxicity even at 1000 nM, whereas ITF2357 was toxic beginning at 200 nM.

*A Comparison of the Effect of ITF2357 with That of ITF3056 on LPS-induced IL-1$\beta$ Steady State mRNA Levels*—As shown in Fig. 4*A*, at 50 nM, IL-1$\beta$ mRNA was reduced by nearly 70% by ITF2357. However, as shown above, at 500 nM, the reduction in mRNA is due to cell injury. Although ITF3056 reduced IL-1$\beta$ mRNA levels dose-dependently, the reduction did not reach significance. Fig. 4*B* also shows the reduction of secreted IL-1$\beta$ in the same cultures. Unlike ITF2357, the inhibitory effect of ITF3056 on mRNA levels as well as secretion of IL-1$\beta$ is linear and without significant cell death.

*Effect of ITF3056 on LPS-induced TNF$\alpha$ Secretion and Gene Expression Compared with ITF2357*—Fig. 5*A* (*left*) depicts the dose-response of ITF2357 inhibition of secreted TNF$\alpha$ following 24-h LPS stimulation. As shown, the greater reductions were at 50 and 100 nM, but at 200, 500, and 1000 nM, increasing levels of TNF$\alpha$ are present, suggesting cell injury. Starting at 50 nM, there is a progressive reduction of TNF$\alpha$ in the presence of ITF3056 with inhibition of 75% at 500 nM and 85% at 1000 nM (Fig. 5*A*, *right*). In a separate PBMCs culture, 20-h LPS-induced TNF$\alpha$ mRNA levels were also determined. There was a reduction in TNF$\alpha$ mRNA of 85% at 50 nM ITF2357 (Fig. 5*B*, *left*). ITF3056 also suppressed TNF$\alpha$ gene expression starting at 100 nM and dose-dependently reduced TNF$\alpha$ mRNA levels by 80% at 1000 nM (Fig. 5*B*, *right*).

*Effect of ITF3056 on LPS-induced IL-6 Secretion and Gene Expression Compared with ITF2357*—ITF2357 suppresses the production of IL-6 in PBMCs stimulated with TLR agonists as well as the combination of IL-12 plus IL-18 (11). As shown in Fig. 6*A* (*left*), IL-6 secretion decreased to 50% at 50 nM ITF2357, but at 100 and 200 nM, there was no reduction. The reductions at 500 and 1000 nM (70 and 80%) are probably due to cell death. The effect of the HDAC8 inhibitor ITF3056 is shown in Fig. 6*A* (*right*) and reveals a linear dose response with maximal reduction of 60% at 1000 nM. In Fig. 6*B* (*left*), the levels of LPS-induced IL-6 mRNA in a 20-h PBMC culture (as in Fig. 5*B*) treated with ITF2357 parallel those of the protein. There is a reduced level at 50 and 100 nM, but the reductions at higher concentrations are related to cell death. In contrast, in PBMCs exposed to ITF3056, the steady state levels of IL-6 mRNA exhibit the same linear dose-response curve with a 50% reduction at 1000 nM, and the mRNA levels parallel those of the protein (Fig. 6*B*, *right*).

*The Effects of ITF Analogues 2357 and 3056 on Candida-induced Cytokine Secretion*—We next assessed the T-cell population employing antigen recall using heat-killed *C. albicans.* There are two components of the *C. albicans* cell wall: an outer layer that is composed of glycoproteins and an inner layer that contains polysaccharides. Immune responses can be induced by components from the outer layer of the cell wall but also by components from the inner layer. Several classes of pattern recognition receptors have been implicated in the recognition of the *Candida* pathogen-associated molecular patterns and the
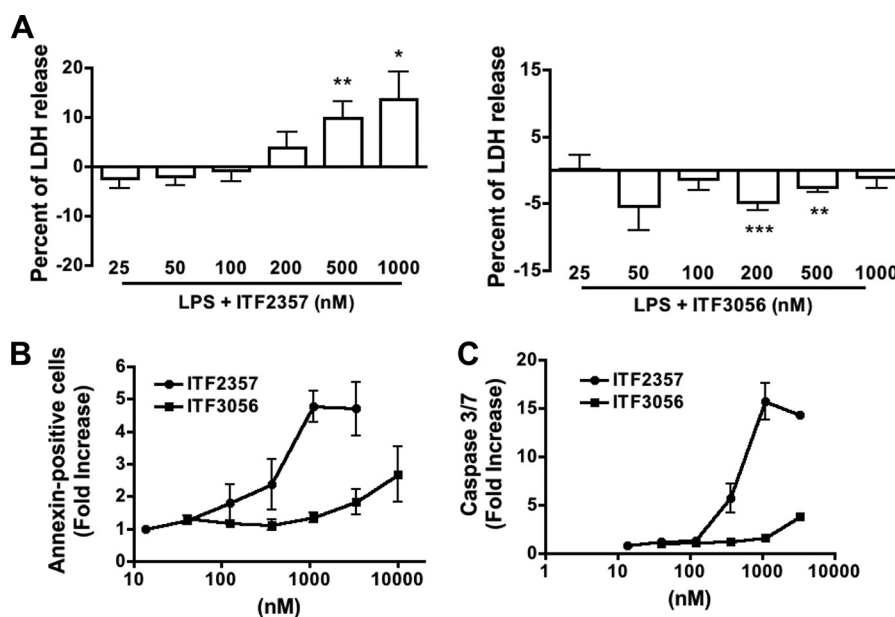
FIGURE 3. **Cytotoxicity differences between ITF2357 and ITF3056.** *A*, mean ± S.E. percentage change of LPS-induced LDH release with increasing concentrations of ITF2357 (*left*) or ITF3056 (*right*) in nine donors derived from data shown in Fig. 1. ***, $p < 0.001$; **, $p < 0.01$; *, $p < 0.05$, compared with LPS alone. *B*, apoptosis and necrosis in monocytes by annexin V/PI staining. Purified monocytes (see "Experimental Procedures") in RPMI were incubated with increasing concentrations of ITF2357 or ITF3056 in the presence of LPS. After 24 h, the percentage of annexin V and PI-positive cells was determined. *C*, 24 h mean ± S.E. caspase-3/7 activation in purified monocytes incubated with increasing concentrations of ITF2357 or 3056 in the presence of LPS ($n = 3$ donors). The data of *B* and *C* are expressed as mean -fold increase compared with monocytes without ITF2357 or ITF3056.
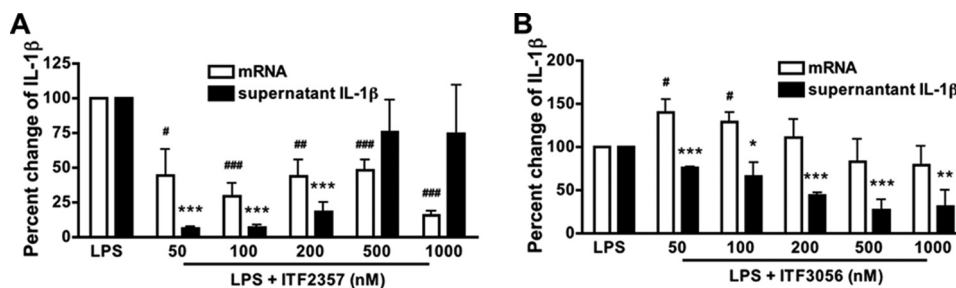


FIGURE 4. **Comparison of the effect of ITF2357 with that of ITF3056 on LPS-induced IL-1$\beta$ steady state mRNA levels.** Shown is dose response of ITF2357 (*A*) and ITF3056 (*B*) in PBMC cultured in a 24-well plate with 10 ng/ml LPS for 20 h. Shown is mean ± S.E. percentage change of LPS-induced IL-1$\beta$ mRNA levels compared with the corresponding supernatant levels of mature IL-1$\beta$ with increasing concentrations. $n = 4$ donors; ### or ***, $p < 0.001$; ## or **, $p < 0.01$; # or *, $p < 0.05$, compared with LPS alone.

induction of innate host responses. These include the Toll-like receptors (TLR2/4/9); the C-type lectin receptors, such as dectin-1/2 and the macrophage mannose receptor; and the NOD-like receptors (27, 37). In this model, there is a requirement for activation of the monocyte and IL-1 dependence (28, 38, 39). Both ITF2357 and ITF3056 reduced *Candida*-induced IL-1$\beta$ and TNF$\alpha$ secretion (Fig. 7*A*). IFN$\gamma$ in the same cultures was reduced for both ITF2357 and ITF3056 (Fig. 7*B*).

*Suppression of Anti-CD3/28-induced IL-1$\beta$ and TNF$\alpha$ by HDAC Inhibition*—Anti-CD3 together with anti-CD28 is widely used to trigger T cells via the T-cell receptor and CD28 co-stimulatory signal (29, 37, 40), thereby mimicking T cell activation during antigen presentation. During a 5-day co-culture with PBMCs, T cells are activated by anti-CD3/28 and induce production of macrophage proinflammatory cytokines, such as IL-1$\beta$ and TNF$\alpha$ (29). As shown in Fig. 8*A*, ITF2357 significantly inhibited anti-CD3/28-induced TNF$\alpha$ secretion in PBMCs by 75% but not IL-1$\beta$ (Fig. 8*A*, *left*). The reduction by ITF3056 of IL-1$\beta$ and TNF$\alpha$ secretion was observed at 100 nM and higher (Fig. 8*A*, *right*). We also measured anti-CD3/28-

induced IFN$\gamma$ in the same cultures and observed partial inhibition for ITF3056 but not ITF2357 (Fig. 8*B*). At 500 nM ITF2357, there is significant cell death (see Fig. 3).

*Effect of ITF3056 on Cytokine Production during Endotoxemia*—The ability of ITF3056 to affect circulating TNF$\alpha$ and IL-1$\beta$ following LPS challenge was assessed. ITF3056 at 0.1, 1, and 10 mg/kg was injected intraperitoneally into mice 1 h before an intraperitoneal injection of LPS (2.5 mg/kg). After 90 min, the mice were sacrificed, and blood was collected. ITF2357 at 10 mg/kg was used as a positive control and, as expected, reduced serum TNF$\alpha$ by 60%. Strikingly, pretreatment of ITF3056 starting at 0.1 mg/kg significantly reduced the circulating TNF$\alpha$ by nearly 90% (Fig. 9*A*). To achieve a significant increase in serum IL-1$\beta$ production, a higher dose of LPS was injected (10 mg/kg), and blood was collected after 4 h. ITF3056 suppressed circulating IL-1$\beta$ linearly, by 45% at 4 mg/kg, 70% at 8 mg/kg, and more than 80% at 16 mg/kg (Fig. 9*B*). Similarly, when pretreated with lower doses of ITF3056 (1 or 5 mg/kg), there was a 22% reduction for 1 mg/kg and 40% for 5 mg/kg.
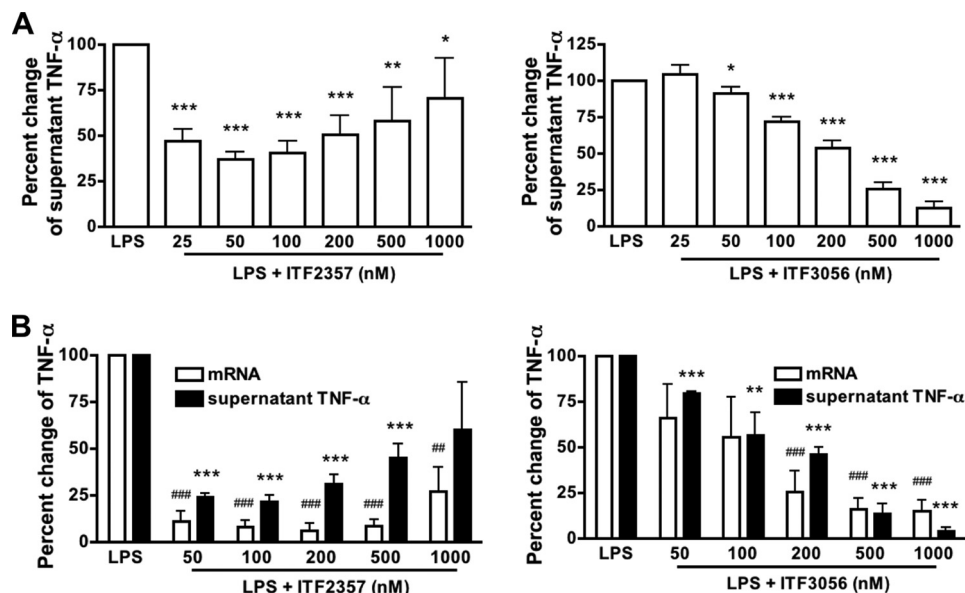
FIGURE 5. **Comparison of the effect of ITF2357 with that of ITF3056 on LPS-induced TNFα secretion and steady state mRNA levels.** *A*, mean ± S.E. percentage change from LPS-induced TNFα secreted (472 ± 149 pg/ml, *n* = 15 donors) with increasing concentrations of ITF2357 (*left*) or ITF3056 (*right*). The cells were seeded on 96-well plates with $0.5 \times 10^6$ PBMCs/well and stimulated with or without 10 ng/ml LPS for 24 h before the supernatant was collected for cytokine measurement. Data are derived from nine donors shown in Fig. 1 with an additional six donors (15 total donors). *B*, mean ± S.E. percentage change from LPS-induced TNFα mRNA synthesis and the corresponding supernatant TNFα with increasing concentrations of ITF2357 (*left*) or ITF3056 (*right*) (*n* = 4 donors). For this study, $3 \times 10^6$ PBMCs were seeded on a 24-well plate with or without 10 ng/ml LPS for 20 h. For all *panels*, ### or ***, $p < 0.001$; ## or **, $p < 0.01$; # or *, $p < 0.05$, compared with LPS alone.
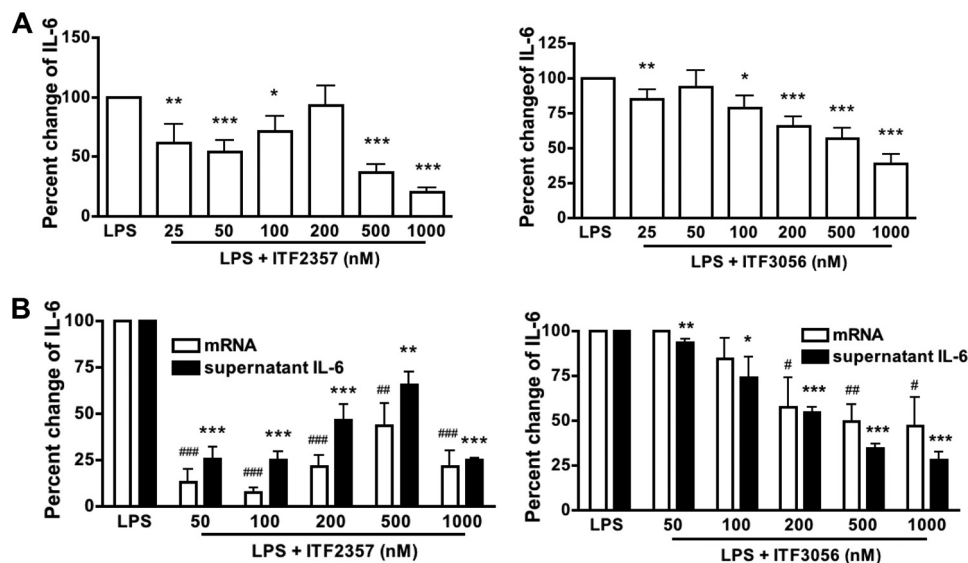


FIGURE 6. **Comparison of the effect of ITF2357 with that of ITF3056 on LPS-induced IL-6 secretion and steady state mRNA synthesis.** *A*, mean ± S.E. percentage change from LPS-induced supernatant IL-6 (22,569 ± 8149 pg/ml, *n* = 15 donors) with increasing concentrations of ITF2357 (*left*) or ITF3056 (*right*). Data are derived from cultures shown in Fig. 5*A*. *B*, mean ± S.E. percentage change from LPS-induced IL-6 mRNA synthesis and the corresponding supernatant IL-6 with increasing concentrations of ITF2357 (*left*) or ITF3056 (*right*) (*n* = 4 donors). Data are derived from cultures shown in Fig. 5*B*. For all *panels*, ### or ***, $p < 0.001$; ## or **, $p < 0.01$; # or *, $p < 0.05$, compared with LPS alone.

In parallel, we used an assay of LPS-induced IL-1β secretion from whole blood cultured from ITF3056-pretreated mice and observed a 24 and 23% reduction for 1 and 5 mg/kg. These data are consistent with LPS-stimulated PBMC culture (Fig. 1).

## DISCUSSION

Although HDAC inhibitors have been and are still being developed to treat cancer, their ability to reduce the production of cytokines *in vitro* and disease severity in animal models of inflammatory and autoimmune conditions (as reviewed in Ref. 9) has prompted renewed interest in compounds that target specific HDACs. It is expected that monospecific inhibition of HDACs will offer optimal safety and efficacy, depending on the dominant cell type or mechanism in a particular disease (9). In this present study, we have compared ITF2357 with the analog ITF3056 on cytokine production as well as gene expression in freshly obtained primary human PBMC. ITF2357 inhibits several HDACs (both class I and class II HDACs), but ITF3056 is unique in that it is highly specific for inhibition of HDAC8.
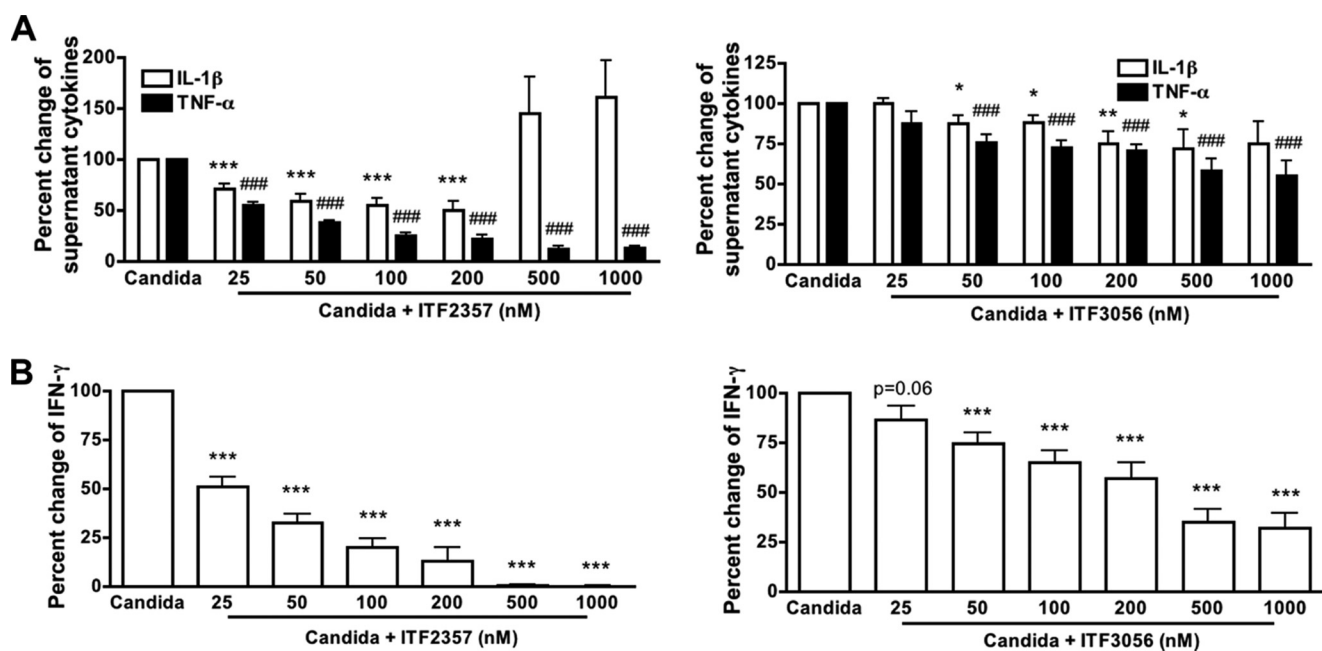
**FIGURE 7. Comparison of ITF2357 with the analog ITF3056 on *Candida*-induced cytokines.** Supernatants from PBMC were cultured in a 96-round bottom well plate and stimulated with heat-killed *C. albicans* for 5 days. *A*, mean ± S.E. percentage change from *Candida*-induced IL-1$\beta$ or TNF$\alpha$ with increasing concentrations of ITF2357 (*left*) or ITF3056 (*right*). *B*, mean ± S.E. percentage change from *Candida*-induced IFN$\gamma$ with increasing concentrations of ITF2357 (*left*) or ITF3056 (*right*). $n = 6$ donors; ### or ***, $p < 0.001$; ## or **, $p < 0.01$; # or *, $p < 0.05$, compared with *Candida* alone.
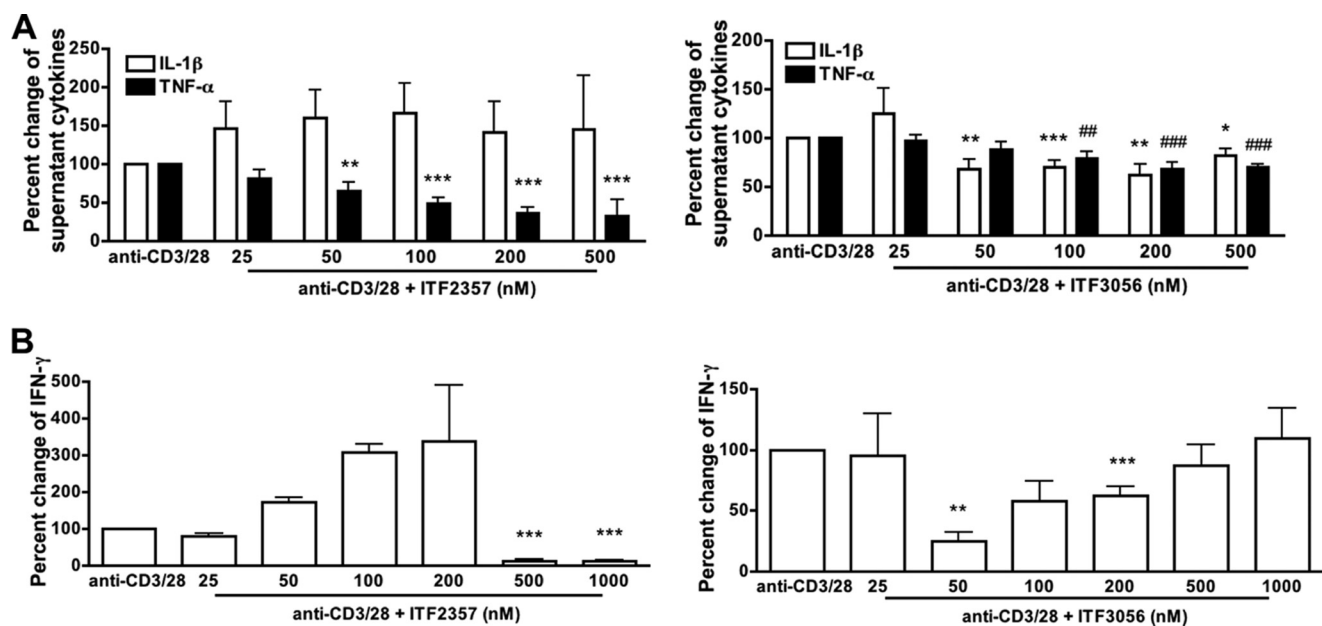


**FIGURE 8. Comparison of the effect of ITF2357 with that of ITF3056 on anti-CD3/28-induced cytokine production.** Cells were cultured with the combination of 5 $\mu$g/ml anti-CD3 plus 1 $\mu$g/ml anti-CD28 for 5 days. *A*, mean ± S.E. percentage change from anti-CD3/28-induced secretion of IL-1$\beta$ or TNF$\alpha$ as measured in the supernatants with increasing concentrations of ITF2357 (*left*) or ITF3056 (*right*). *B*, mean ± S.E. percentage change from anti-CD3/28-induced IFN$\gamma$ with increasing concentrations of ITF2357 (*left*) or ITF3056 (*right*). $n = 5$ donors; ### or ***, $p < 0.001$; ## or **, $p < 0.01$; # or *, $p < 0.05$, compared with anti-CD3/28 alone.

Suppression of cytokine production by ITF3056 compared with that of the pan-HDAC inhibitor ITF2357 was evaluated in PBMCs from the same donor in the same cultures.

One important difference between ITF2357 and ITF3056 is the lack of cell injury by ITF3056. We have reported that concentrations of ITF2357 of 250 nM or higher are injurious to PBMCs, as determined by LDH release as well as annexin staining (11), and presently confirm this observation. Measurements with annexin V staining or caspase-3/7 activation also indicated

that concentrations of ITF2357 greater than 250 nM lead to monocyte apoptosis (Fig. 3). In marked contrast, ITF3056 was devoid of cell injury using either assay. In fact, at 200 nM, PBMCs exposed to ITF3056 released less LDH compare with the LPS alone, suggesting that ITF3056 may enhance cell survival under these conditions. Therefore, the reductions in cytokine production as well as gene expression by ITF3056 at 1000 nM can be assumed to be due to HDAC inhibition and independent of cell injury.
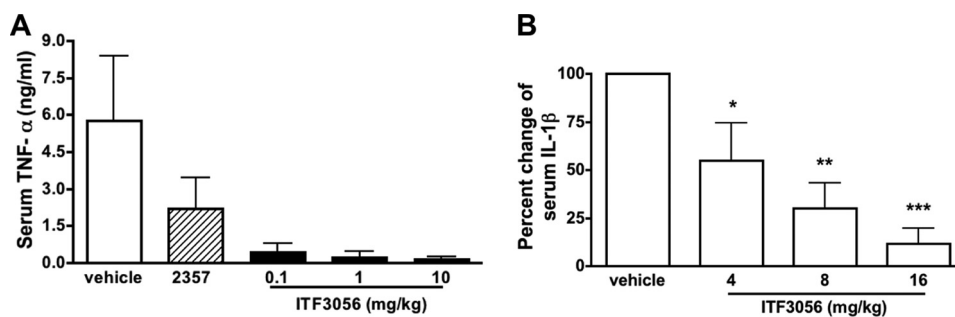
FIGURE 9. **Effect of ITF3056 on *in vivo* endotoxemia-induced cytokine production.** *A*, mean serum TNFα levels of ITF2357 (10 mg/kg)- or ITF3056-treated mice (5 mice/group) 90 min after intraperitoneal injection of 2.5 mg/kg LPS. *B*, mean ± S.E. percentage change of plasma IL-1β from ITF3056-treated mice 4 h after intraperitoneal injection of 10 mg/kg LPS compared with vehicle-treated mice (5 mice/group).

The other notable difference between ITF2357 and ITF3056 is the dose-response relationship. For each cytokine or cytokine gene expression, ITF3056 consistently exhibited a linear decrease to 1000 nM. On the other hand, ITF2357, which consistently inhibited cytokines at 25, 50, and 100 nM, failed to inhibit at 200 nM. This loss in inhibition can be observed in Figs. 1 and 5, for IL-1β and TNFα, respectively. This effect of ITF2357 is probably due to cell injury in that higher concentrations increase the release of LDH (Fig. 3A) and therefore leakage of the IL-1β precursor from the cell. Because the intracellular levels of the IL-1β precursor are markedly low at these higher concentrations (Fig. 1D), the increase in secreted IL-1β is not due to greater caspase-1 processing but rather to the release of the precursor itself. Indeed, we did detect increased release of the IL-1β precursor as a percentage of the total IL-1β produced by the cells, at 500 and 1000 nM ITF2357 (Fig. 1F). Thus, the release of the IL-1β precursor also serves as an indicator of loss of membrane integrity and early cell death.

The increase in the release of the IL-1β precursor observed at high concentrations of ITF2357 is probably not relevant to the effective dose of ITF2357 in the treatment of systemic onset juvenile idiopathic arthritis. The children received a daily oral dose of 1.5 mg/kg, which results in a peak blood level less than 100 nM (18, 20). Animal studies with ITF2357 also demonstrated optimal efficacy of oral ITF2357 in protecting mouse islets from streptozotocin toxicity at 1.25 and 2.5 mg/kg. *In vitro*, ITF2357 at 62.5 and 125 nM reduced cytokine-induced toxicity in rat and mouse beta cells (17, 41). In the non-obese diabetic mouse model of Type 1 diabetes, ITF2357 added to the drinking water prevented the spontaneous development of diabetes (6). The daily dose of ITF2357 in that study was calculated at 1 mg/kg. Therefore, the efficacy of ITF2357 is observed at concentrations considerably less than 200 nM both *in vitro* and *in vivo*. In contrast, ITF3056 *in vitro* at 1000 nM is not toxic.

Following LPS stimulation of freshly obtained human PBMCs, activated caspase-1 cleaves the IL-1β precursor, and the processed IL-1β, together with the uncleaved precursor as well as other contents of the secretory lysosomes, is released by exocytosis in the absence of cell death (42). Although ITF2357 inhibits LPS-induced IL-1β release by preventing exocytosis of IL-1β-containing secretory lysosomes (16), ITF2357 does not directly inhibit the enzymatic activity of caspase-1 (11, 16). In the present study, we measured caspase-1 activity in the cell lysates from ITF2357- and ITF3056-treated PBMC and found

that after 24 h, but not after 4 h, ITF2357 at 25 nM significantly reduced LPS-induced caspase-1 activity by 50% (Fig. 2), most likely due to a reduction in the amount of the enzyme. Although ITF3056 at 1000 nM had no effect on caspase-1 activity in cell lysates, the analog reduced the level of intracellular IL-1β precursor (Fig. 1D), which may partially explain the reduction in mature IL-1β secreted into the extracellular space.

We also observed a significant inhibition of IL-1β steady state mRNA synthesis by ITF2357 in LPS-stimulated PBMCs after 24 h (Fig. 4A). The percentage reduction in IL-1β mRNA at 100 nM is 70%, which differs from a former study in which ITF2357 did not affect LPS-induced IL-1β mRNA levels as assessed by Northern blot analysis (11). In contrast, ITF3056 exhibited non-significant reductions in IL-1β mRNA levels with only 20% at 1000 nM. Nevertheless, there was a 40% reduction in IL-1β secretion at 200 nM and 80% at 1000 nM (Figs. 1C and 4B).

Similar to the previous study (11), we observed a reduction in mRNA levels of TNFα by ITF2357 (Fig. 5B). ITF3056 reduced LPS-induced TNFα and IL-6 mRNA synthesis in parallel to cytokine secretion (Figs. 5B and 6B). A marked (80%) reduction in TNFα mRNA synthesis and nearly 95% reduction in its secretion were observed. For IL-6, mRNA levels were reduced by 50%, and secretion of the cytokine was reduced by 70%. ITF2357 also inhibited IL-6 mRNA synthesis (Fig. 6B, *left*), but similar to its reduction in IL-6 secretion, the inhibition is observed at the lower concentrations of 50 and 100 nM.

In addition to the LPS-induced cytokines, we also observed significant inhibition of *Candida*-induced release of IL-1β, TNFα, and IFNγ by both ITF2357 and ITF3056 (Fig. 7). Because *Candida* activates glucan and mannose receptors as well as Toll-like receptors (37), it was not surprising that we observed similar trends in the reduction of IL-1β and TNFα induced by *Candida* and LPS. ITF2357 had been shown to inhibit LPS- as well as IL-12/IL-18-induced IFNγ but not anti-CD3-induced IFNγ (11). Here, we demonstrate that both ITF2357 and ITF3056 reduced *Candida*-induced IFNγ but not by anti-CD3/28 antibodies, which directly stimulate T cells (Figs. 7B and 8B). These consistent data indicate that the *Candida*-induced IFNγ is macrophage-dependent and that the effects of ITF2357 and ITF3056 are mainly on macrophages in the PBMC culture. Although we detected a low level of inhibition by ITF3056 on anti-CD3/28-induced IL-1β and TNFα (Fig. 8A), the effect is probably through an interaction between

T cells and macrophages. In the 5-day culture of PBMCs, which is a mixed population of monocytes and lymphocytes, there is prolonged interaction between macrophages and T cells. For example, IL-18 and IL-12 secreted by activated macrophages could further activate the T cells in the co-culture to induce IFN$\gamma$ production (32). In fact, ITF2357 inhibits IL-18- and IL-12-induced IFN$\gamma$ in PBMCs, with a 50% reduction at 25 n$\text{M}$ (11).

We tested the *in vivo* effect of ITF2357 and ITF3056 on circulating IL-1$\beta$ and TNF$\alpha$ after LPS challenge. Previous studies showed that ITF2357 reduces LPS-induced circulating TNF$\alpha$ (11), which was confirmed in the present study. However, ITF3056 was highly effective in reducing LPS-induced plasma TNF$\alpha$ levels at low doses of 0.1 mg/kg (Fig. 9*A*). The exact differences between the *in vitro* and *in vivo* effects of ITF3056 are not clear. However, consistent with the *in vitro* study, a linear dose-response relationship is again observed in IL-1$\beta$ production *in vivo* (Fig. 9).

*Note Added in Proof—Maria Luisa Moras' contributions to this article fulfill the JBC authorship criteria, but her authorship was inadvertently omitted from the version of the article that was published on December 1, 2014 as a Paper in Press.*

## REFERENCES

1. Khan, N., Jeffers, M., Kumar, S., Hackett, C., Boldog, F., Khramtsov, N., Qian, X., Mills, E., Berghs, S. C., Carey, N., Finn, P. W., Collins, L. S., Tumber, A., Ritchie, J. W., Jensen, P. B., Lichenstein, H. S., and Sehested, M. (2008) Determination of the class and isoform selectivity of small-molecule histone deacetylase inhibitors. *Biochem. J.* **409,** 581–589

2. Bertos, N. R., Wang, A. H., and Yang, X. J. (2001) Class II histone deacetylases: structure, function, and regulation. *Biochem. Cell Biol.* **79,** 243–252

3. Gregoretti, I. V., Lee, Y. M., and Goodson, H. V. (2004) Molecular evolution of the histone deacetylase family: functional implications of phylogenetic analysis. *J. Mol. Biol.* **338,** 17–31

4. Marks, P. A., and Breslow, R. (2007) Dimethyl sulfoxide to vorinostat: development of this histone deacetylase inhibitor as an anticancer drug. *Nat. Biotechnol.* **25,** 84–90

5. Icardi, L., De Bosscher, K., and Tavernier, J. (2012) The HAT/HDAC interplay: multilevel control of STAT signaling. *Cytokine Growth Factor Rev.* **23,** 283–291

6. Christensen, D. P., Gysemans, C., Lundh, M., Dahllöf, M. S., Noesgaard, D., Schmidt, S. F., Mandrup, S., Birkbak, N., Workman, C. T., Piemonti, L., Blaabjerg, L., Monzani, V., Fossati, G., Mascagni, P., Paraskevas, S., Aikin, R. A., Billestrup, N., Grunnet, L. G., Dinarello, C. A., Mathieu, C., and Mandrup-Poulsen, T. (2014) Lysine deacetylase inhibition prevents diabetes by chromatin-independent immunoregulation and beta-cell protection. *Proc. Natl. Acad. Sci. U.S.A.* **111,** 1055–1059

7. Dinarello, C. A. (2010) Anti-inflammatory agents: present and future. *Cell* **140,** 935–950

8. Marks, P., Rifkind, R. A., Richon, V. M., Breslow, R., Miller, T., and Kelly, W. K. (2001) Histone deacetylases and cancer: causes and therapies. *Nat. Rev. Cancer* **1,** 194–202

9. Dinarello, C. A., Fossati, G., and Mascagni, P. (2011) Histone deacetylase inhibitors for treating a spectrum of diseases not related to cancer. *Mol. Med.* **17,** 333–352

10. Leoni, F., Zaliani, A., Bertolini, G., Porro, G., Pagani, P., Pozzi, P., Donà, G., Fossati, G., Sozzani, S., Azam, T., Bufler, P., Fantuzzi, G., Goncharov, I., Kim, S. H., Pomerantz, B. J., Reznikov, L. L., Siegmund, B., Dinarello, C. A., and Mascagni, P. (2002) The antitumor histone deacetylase inhibitor sub-eroylanilide hydroxamic acid exhibits antiinflammatory properties via suppression of cytokines. *Proc. Natl. Acad. Sci. U.S.A.* **99,** 2995–3000

11. Leoni, F., Fossati, G., Lewis, E. C., Lee, J. K., Porro, G., Pagani, P., Modena, D., Moras, M. L., Pozzi, P., Reznikov, L. L., Siegmund, B., Fantuzzi, G., Dinarello, C. A., and Mascagni, P. (2005) The histone deacetylase inhibitor ITF2357 reduces production of pro-inflammatory cytokines in vitro and systemic inflammation *in vivo*. *Mol. Med.* **11,** 1–15

12. Skov, S., Rieneck, K., Bovin, L. F., Skak, K., Tomra, S., Michelsen, B. K., and Ødum, N. (2003) Histone deacetylase inhibitors: a new class of immunosuppressors targeting a novel signal pathway essential for CD154 expression. *Blood* **101,** 1430–1438

13. Mishra, N., Reilly, C. M., Brown, D. R., Ruiz, P., and Gilkeson, G. S. (2003) Histone deacetylase inhibitors modulate renal disease in the MRL-lpr/lpr mouse. *J. Clin. Invest.* **111,** 539–552

14. Reddy, P., Maeda, Y., Hotary, K., Liu, C., Reznikov, L. L., Dinarello, C. A., and Ferrara, J. L. (2004) Histone deacetylase inhibitor suberoylanilide hydroxamic acid reduces acute graft-*versus*-host disease and preserves graft-*versus*-leukemia effect. *Proc. Natl. Acad. Sci. U.S.A.* **101,** 3921–3926

15. Reilly, C. M., Mishra, N., Miller, J. M., Joshi, D., Ruiz, P., Richon, V. M., Marks, P. A., and Gilkeson, G. S. (2004) Modulation of renal disease in MRL/lpr mice by suberoylanilide hydroxamic acid. *J. Immunol.* **173,** 4171–4178

16. Carta, S., Tassi, S., Semino, C., Fossati, G., Mascagni, P., Dinarello, C. A., and Rubartelli, A. (2006) Histone deacetylase inhibitors prevent exocytosis of interleukin-1$\beta$-containing secretory lysosomes: role of microtubules. *Blood* **108,** 1618–1626

17. Lewis, E. C., Blaabjerg, L., Størling, J., Ronn, S. G., Mascagni, P., Dinarello, C. A., and Mandrup-Poulsen, T. (2011) The oral histone deacetylase inhibitor ITF2357 reduces cytokines and protects islet beta cells *in vivo* and *in vitro*. *Mol. Med.* **17,** 369–377

18. Furlan, A., Monzani, V., Reznikov, L. L., Leoni, F., Fossati, G., Modena, D., Mascagni, P., and Dinarello, C. A. (2011) Pharmacokinetics, safety and inducible cytokine responses during a phase 1 trial of the oral histone deacetylase inhibitor ITF2357 (givinostat). *Mol. Med.* **17,** 353–362

19. Vojinovic, J., and Damjanov, N. (2011) HDAC inhibition in rheumatoid arthritis and juvenile idiopathic arthritis. *Mol. Med.* **17,** 397–403

20. Vojinovic, J., Damjanov, N., D'Urzo, C., Furlan, A., Susic, G., Pasic, S., Iagaru, N., Stefan, M., and Dinarello, C. A. (2011) Safety and efficacy of an oral histone deacetylase inhibitor in systemic onset juvenile idiopathic arthritis. *Arthritis Rheum.* **63,** 1452–1458

21. Choi, S. W., Braun, T., Chang, L., Ferrara, J. L., Pawarode, A., Magenau, J. M., Hou, G., Beumer, J. H., Levine, J. E., Goldstein, S., Couriel, D. R., Stockerl-Goldstein, K., Krijanovski, O. I., Kitko, C., Yanik, G. A., Lehmann, M. H., Tawara, I., Sun, Y., Paczesny, S., Mapara, M. Y., Dinarello, C. A., DiPersio, J. F., and Reddy, P. (2014) Vorinostat plus tacrolimus and mycophenolate to prevent graft-*versus*-host disease after related-donor reduced-intensity conditioning allogeneic haemopoietic stem-cell transplantation: a phase 1/2 trial. *Lancet Oncol.* **15,** 87–95

22. Matalon, S., Palmer, B. E., Nold, M. F., Furlan, A., Kassu, A., Fossati, G., Mascagni, P., and Dinarello, C. A. (2010) The histone deacetylase inhibitor ITF2357 decreases surface CXCR4 and CCR5 expression on CD4(+) T-cells and monocytes and is superior to valproic acid for latent HIV-1 expression *in vitro*. *J. Acquir. Immune Defic. Syndr.* **54,** 1–9

23. Rasmussen, T. A., Schmeltz Søgaard, O., Brinkmann, C., Wightman, F., Lewin, S. R., Melchjorsen, J., Dinarello, C., Østergaard, L., and Tolstrup, M. (2013) Comparison of HDAC inhibitors in clinical development: effect on HIV production in latently infected cells and T-cell activation. *Hum. Vaccin. Immunother.* **9,** 993–1001

24. Barton, K. M., Archin, N. M., Keedy, K. S., Espeseth, A. S., Zhang, Y. L., Gale, J., Wagner, F. F., Holson, E. B., and Margolis, D. M. (2014) Selective HDAC inhibition for the disruption of latent HIV-1 infection. *PLoS One* **9,** e102684

25. Manson McManamy, M. E., Hakre, S., Verdin, E. M., and Margolis, D. M. (2014) Therapy for latent HIV-1 infection: the role of histone deacetylase inhibitors. *Antivir. Chem. Chemother.* **23,** 145–149

26. Archin, N. M., Bateson, R., Tripathy, M. K., Crooks, A. M., Yang, K. H., Dahl, N. P., Kearney, M. F., Anderson, E. M., Coffin, J. M., Strain, M. C., Richman, D. D., Robertson, K. R., Kashuba, A. D., Bosch, R. J., Hazuda,

D. J., Kuruc, J. D., Eron, J. J., and Margolis, D. M. (2014) HIV-1 expression within resting CD4+ T cells after multiple doses of vorinostat. *J. Infect. Dis.* **210,** 728–735

27. Gow, N. A., van de Veerdonk, F. L., Brown, A. J., and Netea, M. G. (2012) *Candida albicans* morphogenesis and host defence: discriminating invasion from colonization. *Nat. Rev. Microbiol.* **10,** 112–122

28. van de Veerdonk, F. L., Joosten, L. A., Devesa, I., Mora-Montes, H. M., Kanneganti, T. D., Dinarello, C. A., van der Meer, J. W., Gow, N. A., Kullberg, B. J., and Netea, M. G. (2009) Bypassing pathogen-induced inflammasome activation for the regulation of interleukin-1β production by the fungal pathogen *Candida albicans. J. Infect. Dis.* **199,** 1087–1096

29. van de Veerdonk, F. L., Marijnissen, R. J., Kullberg, B. J., Koenen, H. J., Cheng, S. C., Joosten, I., van den Berg, W. B., Williams, D. L., van der Meer, J. W., Joosten, L. A., and Netea, M. G. (2009) The macrophage mannose receptor induces IL-17 in response to *Candida albicans. Cell Host Microbe* **5,** 329–340

30. Rivera, V. R., Gamez, F. J., Keener, W. K., White, J. A., and Poli, M. A. (2006) Rapid detection of *Clostridium botulinum* toxins A, B, E, and F in clinical samples, selected food matrices, and buffer using paramagnetic bead-based electrochemiluminescence detection. *Anal. Biochem.* **353,** 248–256

31. Qiu, Z. J., Ying, Y., Fox, M., Peng, K., Lewin-Koh, S. C., Coleman, D., Good, J., Lowe, J., Rahman, A., Yang, J., Jiang, J., Quarmby, V., and Song, A. (2010) A novel homogeneous Biotin-digoxigenin based assay for the detection of human anti-therapeutic antibodies in autoimmune serum. *J. Immunol. Methods* **362,** 101–111

32. Netea, M. G., Stuyt, R. J., Kim, S. H., Van der Meer, J. W., Kullberg, B. J., and Dinarello, C. A. (2002) The role of endogenous interleukin (IL)-18, IL-12, IL-1β, and tumor necrosis factor-α in the production of interferon-γ induced by *Candida albicans* in human whole-blood cultures. *J. Infect. Dis.* **185,** 963–970

33. Nold, M. F., Nold-Petry, C. A., Zepp, J. A., Palmer, B. E., Bufler, P., and Dinarello, C. A. (2010) IL-37 is a fundamental inhibitor of innate immunity. *Nat. Immunol.* **11,** 1014–1022

34. Kölle, D., Brosch, G., Lechner, T., Lusser, A., and Loidl, P. (1998) Biochemical methods for analysis of histone deacetylases. *Methods* **15,** 323–331

35. Netea, M. G., Nold-Petry, C. A., Nold, M. F., Joosten, L. A., Opitz, B., van der Meer, J. H., van de Veerdonk, F. L., Ferwerda, G., Heinhuis, B., Devesa, I., Funk, C. J., Mason, R. J., Kullberg, B. J., Rubartelli, A., van der Meer, J. W., and Dinarello, C. A. (2009) Differential requirement for the activation of the inflammasome for processing and release of IL-1β in monocytes and macrophages. *Blood* **113,** 2324–2335

36. Levandowski, C. B., Mailloux, C. M., Ferrara, T. M., Gowan, K., Ben, S., Jin, Y., McFann, K. K., Holland, P. J., Fain, P. R., Dinarello, C. A., and Spritz, R. A. (2013) NLRP1 haplotypes associated with vitiligo and autoimmunity increase interleukin-1β processing via the NLRP1 inflammasome. *Proc. Natl. Acad. Sci. U.S.A.* **110,** 2952–2956

37. Cheng, S. C., Joosten, L. A., Kullberg, B. J., and Netea, M. G. (2012) Interplay between *Candida albicans* and the mammalian innate host defense. *Infect. Immun.* **80,** 1304–1313

38. Chedid, L., Parant, M., Parant, F., Lefrancher, P., Choay, J., and Lederer, E. (1977) Enhancement of nonspecific immunity to *Klebsiella pneumoniae* infection by a synthetic immunoadjuvant (*N*-acetylmuramyl-L-alanyl-D-isoglutamine) and several analogs. *Proc. Natl. Acad. Sci. U.S.A.* **74,** 2089–2093

39. Cheng, S. C., van de Veerdonk, F. L., Lenardon, M., Stoffels, M., Plantinga, T., Smeekens, S., Rizzetto, L., Mukaremera, L., Preechasuth, K., Cavalieri, D., Kanneganti, T. D., van der Meer, J. W., Kullberg, B. J., Joosten, L. A., Gow, N. A., and Netea, M. G. (2011) The dectin-1/inflammasome pathway is responsible for the induction of protective T-helper 17 responses that discriminate between yeasts and hyphae of *Candida albicans. J. Leukoc. Biol.* **90,** 357–366

40. Wang, H., Wei, W., Shen, Y. X., Dong, C., Zhang, L. L., Wang, N. P., Yue, L., and Xu, S. Y. (2004) Protective effect of melatonin against liver injury in mice induced by Bacillus Calmette-Guerin plus lipopolysaccharide. *World J. Gastroenterol.* **10,** 2690–2696

41. Lundh, M., Christensen, D. P., Rasmussen, D. N., Mascagni, P., Dinarello, C. A., Billestrup, N., Grunnet, L. G., and Mandrup-Poulsen, T. (2010) Lysine deacetylases are produced in pancreatic beta cells and are differentially regulated by proinflammatory cytokines. *Diabetologia* **53,** 2569–2578

42. Andrei, C., Margiocco, P., Poggi, A., Lotti, L. V., Torrisi, M. R., and Rubartelli, A. (2004) Phospholipases C and A2 control lysosome-mediated IL-1β secretion: implications for inflammatory processes. *Proc. Natl. Acad. Sci. U.S.A.* **101,** 9745–9750